The Journal of Experimental Biology 201, 2691–2699 (1998)
Printed in Great Britain © The Company of Biologists Limited 1998
JEB1600

MECHANICAL PROPERTIES OF THE TADPOLE TAIL FIN

PENNY A. DOHERTY[1], RICHARD J. WASSERSUG[2,*] AND J. MICHAEL LEE[3]

[1]*Department of Biology,* [2]*Department of Anatomy and Neurobiology* and [3]*Division of Biomaterials, Dalhousie University, Halifax, Nova Scotia, Canada B3H 4H7*

*Author for correspondence (e-mail: tadpole@is.dal.ca)

Accepted 14 July; published on WWW 10 September 1998

Summary

The tadpole tail fin is a simple double layer of skin overlying loose connective tissue. Collagen fibres in the fin are oriented at approximately ±45° from the long axis of the tail.

Three tests were conducted on samples of the dorsal tail fin from 6–10 *Rana catesbeiana* tadpoles to establish the fin's viscoelastic properties under (1) large-deformation cyclic loading at 1 and 3 Hz, (2) small-deformation forced vibration at 1 and 3 Hz, and (3) stress relaxation under a 0.1 s loading time. The fin was very fragile, failing easily under tensile loads less than 7 g. It was also strikingly viscoelastic, as demonstrated by 72±1 % hysteresis loss (at 3 Hz), 16±3 % stress remaining after 100 s of stress relaxation and a phase angle of 18±1° in forced vibration. As a consequence of its viscoelastic properties, the fin was three times stiffer in small than in large deformation. This may account for the ability of the fin to stay upright during normal undulatory swimming, despite the absence of any skeletal support.

Tadpoles in nature are often found with damaged tails. We suggest that the unusually viscoelastic and fragile nature of the fin helps tadpoles escape the grasp of predators. Because the fin deforms viscoelastically and tears easily, tadpoles can escape predators and survive otherwise lethal attacks with only minor lacerations to the fin. Recent studies have shown that certain tadpoles develop taller fins in the presence of predators. This developmental plasticity is consistent with the tail fin acting as a protective but expendable 'wrap' around the core muscle tissue.

Key words: *Rana catesbeiana*, anuran larva, tadpole, tail fin, predation, locomotion, swimming, mechanics, viscoelasticity.

Introduction

The tadpole tail fin is one of the simplest, but strangest, fins in the vertebrate world. It is a laterally compressed structure that circumscribes dorsally and ventrally the muscular core of the tail. In contrast to the vast majority of aquatic vertebrates, which are actinopterygian fishes defined by the presence of either cartilaginous or bony fin rays, the tadpole tail fin completely lacks skeletal support (Wassersug, 1989).

Direct observation of the tail fin in resting or swimming tadpoles indicates that the majority of the fin is, however, stiff enough to remain erect most of the time. Ciné films of tadpoles swimming at high velocity similarly reveal little or no deflection of the fin out of the vertical plane, even when the tail is bending rapidly (Liu *et al.* 1997). Thus, the fin (at least its anterior portion as far caudal as the deepest portion of the fin) is stiff enough to act as a flexible vertical plate during undulatory locomotion, providing a surface for the generation of thrust (Wassersug and Hoff, 1985; Wassersug, 1989; Liu *et al.* 1997).

At the same time, the tadpole tail fin remains a delicate structure. Herpetologists learn quickly that the tadpole tail fin tears easily when grasped with forceps. Tadpoles in nature are commonly found with damaged and torn tail fins (Caldwell, 1982). Both invertebrates and vertebrates often take pieces out of the tail of tadpoles (Morin, 1985; Caldwell, 1994), leading to estimates of tail damage in natural populations exceeding 50 % (Caldwell, 1982). We have, in fact, found bullfrog tadpoles (*Rana catesbeiana*) in a natural population where 88 % of the individuals (N=98) had some tail fin injury (J. Blair and R. Wassersug, personal observation). Such high injury rates suggest that the tadpole tail fin should perform poorly under tensile loading. However, the mechanical properties of the fin have never been tested in any anuran larvae.

Pliant soft connective tissues, such as the tadpole tail fin, are typically subjected to biaxial tensile and bending deformations. They will not support compression in bending and will deform (i) by tensile extension and internal shear or less commonly (ii) in tensile extension and by buckling on the concave surface (Wainwright *et al.* 1976). In the present paper, we have made the pragmatic choice to examine the uniaxial tensile properties of the tail fin only. Measurement of bending properties in very thin, pliant structures, such as the isolated tail fin, are technically difficult and rarely attempted (Vesely and Boughner, 1985).

Like all soft connective tissues, the tadpole tail fin can be

expected to show viscoelastic behaviour. Viscoelastic materials display some balance between the behaviour of an elastic solid (energy storage and return upon loading/unloading) and the behaviour of a viscous liquid (irrecoverable flow, energy lost due to internal friction). Viscoelasticity in tissues is usually assessed in terms of one or more of the following features: (i) hysteresis losses during large-deformation cyclic loading (loading and unloading curves are different); (ii) stress relaxation (a reduction in load under constant extension); (iii) creep (an increase in extension under constant load); or (iv) the phase angle between stress and strain sinusoids during forced small vibrations. Each of these parameters would be zero in a completely elastic material. We note that hysteresis losses and stress relaxation/creep are usually measured under large deformations, where collagen fibres can be expected to sweep through the surrounding viscous gel/sol, whereas forced vibration phase angles are usually measured under small deformations, where this is less likely. Consequently, comparison of parameters i–iii with parameter iv can reveal information about the relative viscoelasticity of the tissue under different scaled deformations.

In this report, we examine the performance of the tadpole dorsal tail fin when subjected to stress/strain, forced vibration and stress relaxation testing. Collectively, these tests show that the tadpole tail fin is fragile, but surprisingly viscoelastic. This unusual combination of properties might result in damage to the tadpole tail when subjected to tensile forces, but ultimately might allow many tadpoles to survive predatory attacks.

Materials and methods

Mechanical testing

Ten premetamorphic *Rana catesbeiana* tadpoles (obtained from Carolina Biological Supply Co., South Carolina, USA) were used for these experiments. They were maintained in the laboratory according to guidelines from the Canadian Council on Animal Care (1984). Tadpoles were all between Gosner (1960) developmental stages 33 and 36 (i.e. mature, free-living tadpoles with small hind limbs) and 6.8±0.17 cm (mean ± S.E.M.) in total length. The mean thickness of their fins was 0.39±0.02 mm.

The tadpoles were anaesthetized individually with an overdose of MS-222. Then 15 mm×5 mm longitudinal strips were removed from the dorsal fin within 10 min of death. Because of the laterally compressed nature of the tail fin, these samples were of nearly constant thickness. The strips were immediately clamped to a nominal gauge length of 10 mm between custom-made, rubber-lined, spring grips that minimized gripping damage to the tissue. Mounted samples were maintained in standing tap water at room temperature (20 °C) typically for no longer than 30 min prior to any mechanical testing.

Mechanical tests for viscoelastic behaviour were performed, as described by Lee *et al.* (1994), on a multiaxial MTS servo-hydraulic testing machine (MTS Systems, Minneapolis, USA). All tests were performed with the samples immersed in an acrylic tissue bath containing standing tap water at room temperature. The sample and tissue grips were mounted between two screw-tightened brass grips. One grip was attached to a 1000 g cantilever load cell (Transducer Techniques), used with a 400 g range cartridge, and the other to a servo-hydraulic actuator. The grips were carefully aligned to ensure uniaxial loading. The testing machine was operated in stroke control (i.e. the extension/time curve was programmed), using the MTS TRAC synthesis system for extension wave forms. Load data were captured using a 400 g cartridge in the conditioning amplifier and transferred to computer *via* a 12-bit A/D card (load resolution 0.2) with 9 μs sampling time (National Instruments, Austin, Texas, USA) in a Macintosh Centris 650 computer running custom-written software (LabVIEW software, National Instruments). Tissue extension was measured from the linear variable differential transformer in the MTS actuator using a 37.5 mm cartridge in the conditioning amplifier and similarly acquired by the computer system. The range cartridge determined the sensitivity of the load and extension measurements as range/4096 (where 4096=12 bits).

To establish gauge length, each fin strip was extended by the servo-hydraulic actuator until an increase in load was observed and then retracted until the load just reached 0 g. This length at 0 g was recorded as the gauge length. An image of the sample was captured using an overhead Cohu CCD video camera with macro zoom lens and a Supermac Video Spigot frame-grabber card in the Macintosh Centris 650 computer. Without altering the magnification, a ruler was placed on the brass grips and its image was similarly recorded to provide a calibration scale.

Three tests were performed on each fin strip: (1) large-deflection cyclic loading to assess stiffness and viscoelastic hysteresis losses, i.e. stress–strain measurements, (2) small-deflection forced vibration, and (3) stress relaxation. Mechanical tests involving cyclic loading were typically performed at 3 Hz because *Rana catesbeiana* tadpoles of approximately the same size and stage as those used used here have a preferred tail beat frequency of approximately 3 Hz during normal voluntary swimming at room temperature (Hoff, 1987). A maximum load of 3 g was chosen pragmatically since the fin samples were extremely fragile and typically failed at loads of 5–7 g. Indeed, despite bevelled grip edges, repeated loading occasionally resulted in failure at the grip edges before all tests could be completed; hence, 10 fins were required to yield a minimum sample of six measurements for forced vibration and stress relaxation. Precise tensile strength measurements were considered unreliable for these friable samples and are not reported here.

Before each test, the test strip was preconditioned with 12 sinusoidal loading cycles between 0 and 3 g at a frequency of 3 Hz to provide a reproducible mechanical state. The cyclic load/elongation response was then measured at 1 and 3 Hz between 0 and 3 g. Testing at 1 Hz was performed to allow a comparison with other tissues tested on the same or similar equipment (Lee *et al.* 1994; Imura *et al.* 1990). The loading time in these tests was half the wave-form period: 1/6 s. One hundred data pairs of load/extension were recorded during each

cycle. Ten specimens underwent large-deformation cyclic loading.

Forced vibration tests were carried out by imposing small sinusoidal extensions at 3 Hz about the tissue extensions corresponding to a mean load of 3 g. The strip was preconditioned as described above, then extended by the application of a mean load of 3 g, and the corresponding extension was recorded. The strip was then vibrated sinusoidally with an amplitude of one-tenth of the total extension about that extension. One hundred data pairs were again recorded for each cycle. Six specimens underwent forced vibration testing.

Stress relaxation tests were performed last. The strip was preconditioned as described above and then extended to a length corresponding to a 3 g load with a loading time of 0.1 s. Once that load had been achieved, the strip was held at the corresponding extension for 100 s and the decay of the load measured. Data were recorded every 2 ms throughout the test. Stress relaxation tests were performed on six specimens.

The thickness of each strip was measured after testing using a Mitutoyo non-rotating thickness gauge (model 7309), as described by Lee and Langdon (1996).

Histology

Samples approximately 5 mm long were cut along the longitudinal axis of the body from the dorsal margin of the dorsal tail fin down to the caudal muscle. These samples were fixed in 10 % neutral-buffered formalin (Fisher Scientific, Toronto). Some samples were split along the ventral/dorsal plane and stained with Picrosirius Red (Sigma-Aldrich, St Louis, USA) to enhance collagen birefringence. No other staining was used. The half-fins were sandwiched between a glass microscope slide and coverslip, and observed in a light microscope equipped with birefringence polarizers. Other fixed samples of fins were dehydrated in a graded series of alcohols, embedded in paraffin, and sectioned using a microtome into 7 μm cross sections. These sections were similarly stained with Picrosirius Red and observed using birefringence microscopy.

Data analysis

The gauge length and width of the unloaded strips were measured using NIH Image software from the digitized images of each strip (US National Institutes of Health; available at http://rsb.info.nih.gov/nih-image/). The gauge length of the strip between the grips was digitized on each side of the strip and averaged to produce a mean gauge length, L_0. The area of the strip was then digitized, and the mean strip width determined by dividing the area by the mean length. The thickness and mean width of the strip were then multiplied to determine a mean cross-sectional area, A_0.

Strain in the fin strips was calculated as the percentage extension of the sample $\Delta L/L_0$, where ΔL is the extension and L_0 is the gauge length measured from the video image. Stress was calculated as $F\boldsymbol{g}/A_0$, where F is the load on the strip, $\boldsymbol{g}$ is the acceleration due to gravity and A_0 is the mean cross-sectional area as calculated above.

Hysteresis, the fractional energy loss during loading/unloading, was calculated from the large-deformation stress–strain curves as the difference between the areas under the loading and unloading curves (the hysteresis loop) divided by the area under the loading curve (the strain energy during loading). It was expressed as a percentage. Using a classic technique, areas corresponding to those under the loading curve and to the hysteresis loop were simply cut out from the paper on which they were printed. The pieces of paper were then weighed and the areas calculated from the masses.

The tangent modulus at a stress of 7.0 kPa was determined by taking a best-fit tangent to the loading arm of the stress–strain curve at this point. The stress of 7.0 kPa was chosen pragmatically because the mean stress during forced vibration (i.e. produced by a mean load of 3 g) was approximately 7.0 kPa. Choosing this value allowed comparison of the moduli from large- and small-deformation testing.

For the forced vibration experiments, data were analyzed as described by Lee *et al.* (1994). To determine the sinusoids of best fit, the stress–time data were fitted using a Levant–Marquart non-linear least-squares method with DeltaGraph 2.0.3 software (DeltaPoint). The applied stress was thus taken to vary with time such that:

$$\sigma(t) = \sigma_m + \sigma_0 \sin(2\pi f t + \alpha), \quad (1)$$

where $\sigma(t)$ is the stress at time t, σ_m is the mean stress, σ_0 is the amplitude of the stress sinusoid curve, f is the frequency in Hz, and α is the phase angle of the stress. The corresponding strain was then similarly fitted as:

$$\varepsilon(t) = \varepsilon_m + \varepsilon_0 \sin(2\pi f t + \beta), \quad (2)$$

where $\varepsilon(t)$ is the strain at time t, ε_m is the mean strain, ε_0 is the amplitude of the sinusoidal strain curve, and β is the phase angle of the strain. Once a close match between the experimental data points and the fitted curves had been obtained, values corresponding to σ_0, ε_0, α and β were saved. The phase lag (ϕ) of the strain behind the stress was calculated from the parameters in these two fitted equations as $\phi=\alpha-\beta$.

The dynamic modulus E^* is a complex number, the ratio of the time-varying sinusoids $\sigma(t)/\varepsilon(t)$. It represents the time-dependent stiffness of the material under vibration. Note that if there were no phase shift between $\sigma(t)$ and $\varepsilon(t)$, then E^* would be a real number, the elastic stiffness of the material. E^* may be expressed in polar notation, consisting of a magnitude $|E^*|$ that represents the dynamic stiffness of the material and a phase angle ϕ by which the strain sinusoid $\varepsilon(t)$ lags behind the stress sinusoid $\sigma(t)$. For an elastic material, ϕ would equal zero. The magnitude of the complex dynamic modulus $|E^*|$ was calculated as the ratio σ_0/ε_0. The two components of the dynamic modulus – the storage modulus, E_S, and the loss modulus, E_L – were calculated from the following equations:

$$E_S = |E^*|\cos\phi, \quad (3)$$

$$E_L = |E^*|\sin\phi, \quad (4)$$

where $E^*=E_S+iE_L$, i being the square root of –1. For a purely elastic material, E_L would equal zero.

For the stress relaxation experiments, the percentage stress remaining was calculated as the ratio of the stress at time t, $\sigma(t)$, to the initial stress when relaxation began (t=0), multiplied by 100. This ratio was plotted on a logarithmic time axis. Care was taken to exclude data that might have been influenced by the relaxation that occurred during the initial extension. After the load had been achieved, data were collected only after a period equal to four times the loading time (Turner, 1983).

Statistical analyses

Descriptive statistics were performed on all the data to obtain means, standard deviations and standard errors of the mean (StatView 4.5, Abacus Concepts). A one-way analysis of variance (ANOVA) was used for stress–strain and hysteresis results where the variable was frequency at 1 and 3 Hz. Data are presented as the mean ± the standard error of the mean (S.E.M.).

Results

Stress–strain response

The tadpole tail fin demonstrated marked viscoelastic behaviour under large-deformation stress–strain tests. A typical stress–strain curve with a hysteresis loop is shown in Fig. 1, and Table 1 summarizes the mechanical properties calculated from stress–strain tests at 1 and 3 Hz. The concave upward shape of the stress–strain curve is typical of other connective tissues. The large hysteresis loops seen at both frequencies indicate that a large fraction of the strain energy during loading was lost to viscoelastic processes. There were

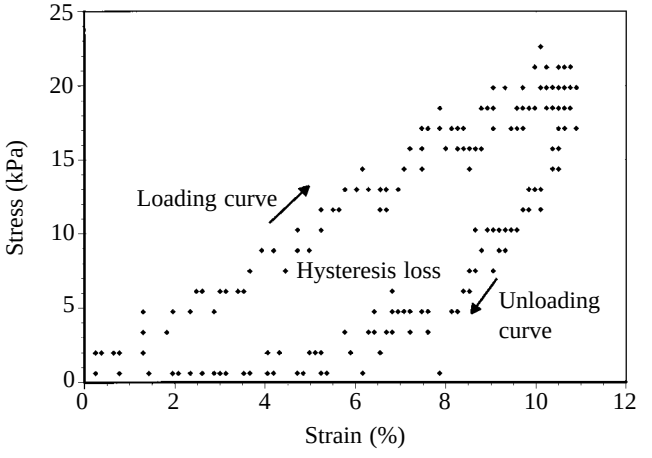

Fig. 1. Typical raw stress–strain curve at 3 Hz for a longitudinal strip of bullfrog (*Rana catesbeiana*) tadpole tail fin. The area under the loading curve is the strain energy per unit volume imparted to the material during loading; i.e. the work done on loading. The area under the unloading curve is the energy per unit volume recovered on unloading. The area within the two curves is the hysteresis loss, calculated as a percentage and shown in Table 1. This value represents the fraction of the loading energy lost to viscous processes. The curve shows that the tadpole tail fin is very viscoelastic in large-deformation cyclic loading.

Table 1. *Effect of frequency on stress–strain responses and hysteresis for large-deformation cyclic loading of the bullfrog tail fin*

	Frequency		
	1 Hz	3 Hz	*P*
Maximum stress under 3 g load (kPa)	16.7±1.5	18.7±1.6	0.4170
Maximum strain under 3 g load (%)	11.0±0.55	12.4±0.95	0.3182
Hysteresis loss (%)	70.0±2.35	72.0±1.14	0.3973
Tangential modulus at 7 kPa stress (kPa)	88.9±9.1	85.1±6.5	0.7405

Values are means ± S.E.M., N=10.
One-way ANOVAs reveal no significant differences between the 1 and 3 Hz test results.

no significant differences in the large-deformation stress–strain responses at the two test frequencies (Table 1).

Forced vibration

The forced vibration data confirmed the viscoelasticity seen in the stress–strain response. Typical raw stress and strain curves and their sinusoids of best fit are shown in Fig. 2. At a mean load stress of approximately 7.0 kPa (6.95±0.38 kPa; N=6), the phase angle (ϕ) was large, ranging from 14 to 21 ° (17.6±1 °). The loss (viscous) modulus E_L was 90±17 kPa, or almost one-third of the storage (elastic) modulus E_S, which averaged 278±39 kPa. Interestingly, the magnitude of the dynamic modulus ($|E^*|$) was 293±42 kPa, which was more than three times larger than the tangential modulus at 7.0 kPa stress, determined in large-deformation stress–strain tests. The fin was therefore significantly stiffer in small deformations (at this stress) than it was in large deformations at the same frequency.

Stress relaxation

The large-deformation viscoelasticity of the fin was further demonstrated by the marked stress relaxation observed (Fig. 3). After the fin had been held at a fixed length for only 0.4 s, the stress had fallen to approximately 60 % of its initial value. By 100 s, only 15 % of the stress remained. Stress relaxation continued throughout the experiment, and extrapolation of the curve in Fig. 3 suggests that the percentage stress remaining might reach zero at approximately 1000 s.

Histology

Birefringence microscopy of the split tadpole fins demonstrated layers of collagen fibres oriented at approximately ±45 ° to the longitudinal axis of the fin (Fig. 4). While there was some local heterogeneity to this structure, it was well-defined from the myotomal muscle through to the free edge of the fin. In cross section, these collagen layers could be seen to form a jacket or sheath surrounding a central space

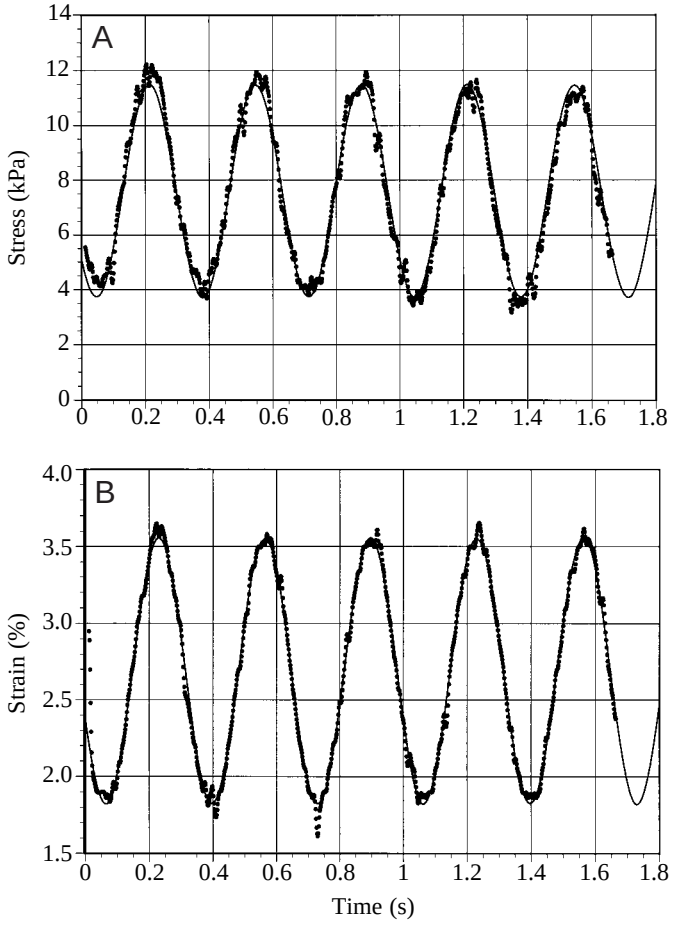

Fig. 2. Raw stress–time (A) and strain–time (B) curves for a longitudinal strip of tadpole tail fin. Superimposed on the data points are the sinusoids of best fit used to calculate the dynamic modulus E^* and the phase angle ϕ between the two sinusoids. The decline in peak and trough stresses with time in A shows that the stress relaxed during vibration about a given mean strain. These data confirm that the tadpole tail fin demonstrates substantial viscoelastic behaviour under small sinusoidal deformations.

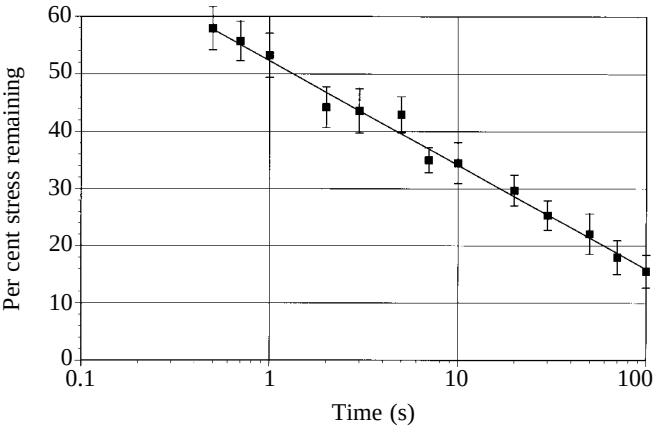

Fig. 3. Mean percentage stress remaining (± standard error of the mean) for N=6 longitudinal strips of tadpole tail fin loaded to 3 g in 0.1 s. Data are shown only for a period equal to four times the loading time to avoid distortions due to relaxation that occurred during loading. The tadpole tail fin loses 85 % of the stress at initial extension in 100 s. % stress remaining=52.5–18.3log$_{10}$(t); r^2=0.99, P<0.0001.

that displayed light connective tissue reinforcement and only a few longitudinal structures (elliptical in cross section) which were outlined in birefringent collagen (Fig. 5).

Discussion

The tail fin is little more than a double layer of skin; i.e. a layer of loose connective tissue covered on both sides by dermis (Yoshizato, 1986). The basement lamella of the dermis is an array of crossed collagen fibres that run obliquely from the long axis of the tadpole (Fig. 4). Such oblique, crossed fibres have been observed in the skin of many aquatic vertebrates (e.g. see references in Hebrank and Hebrank, 1986; Frolich and Schmid, 1991), including anuran larvae (e.g. Overton, 1976; Rosin, 1946), where they can be conspicuous to the naked eye and have even been used for species identification (Berninghausen, 1997). This pattern of fibres has been described by Wainwright *et al.* (1976) as a crossed-fibrillar array and suggests that the fin should have approximately equal strength and stiffness in the vertical and longitudinal directions. Because of the orientation of the collagen fibres, positive fluid pressure within the fin, i.e. in the internal space seen in Fig. 5, may allow the fin to act as a hydrostat (Kier, 1992) and thus gain some stiffness.

Because the tadpole tail fin remains vertically oriented during swimming (see the figures in Wassersug and Hoff, 1985, and discussion in Liu *et al.* 1997), it must be stiff enough to resist major deformation during undulatory locomotion. The crossed-fibrillar arrangement of the collagen fibres in the tadpole tail fin is similar to that seen in the body-wall connective tissue and cuticle of many worm-like animals and several vertebrates (Wainwright *et al.* 1976) and might be involved in controlling the range of shape and movement possible in the fin. However, unlike the 55°44′ fibre angle in the crossed-helical array of cylindrical animals (Kier, 1992), the angle of collagen fibres to the long axis in the laterally flattened tadpole tail fin is approximately 45 °. That 45 ° angle (as opposed to greater or lesser angles) could provide the fin with equivalent support in both the vertical (dorsoventral) and longitudinal (rostrocaudal) directions; i.e. the isotropic structure of the fin suggests isotropic mechanical properties in the orthogonal vertical and longitudinal directions. However, as noted below, mechanical testing of vertically oriented fin strips was not possible.

One of the most striking characteristics of the tadpole tail fin is its marked fragility. We found that the fin could be shredded with forceps almost as easily as wet tissue paper. Therefore, handling and gripping the fin strips for mechanical testing proved difficult. The custom-built rubber grips ultimately used in our study permitted mechanical testing, but

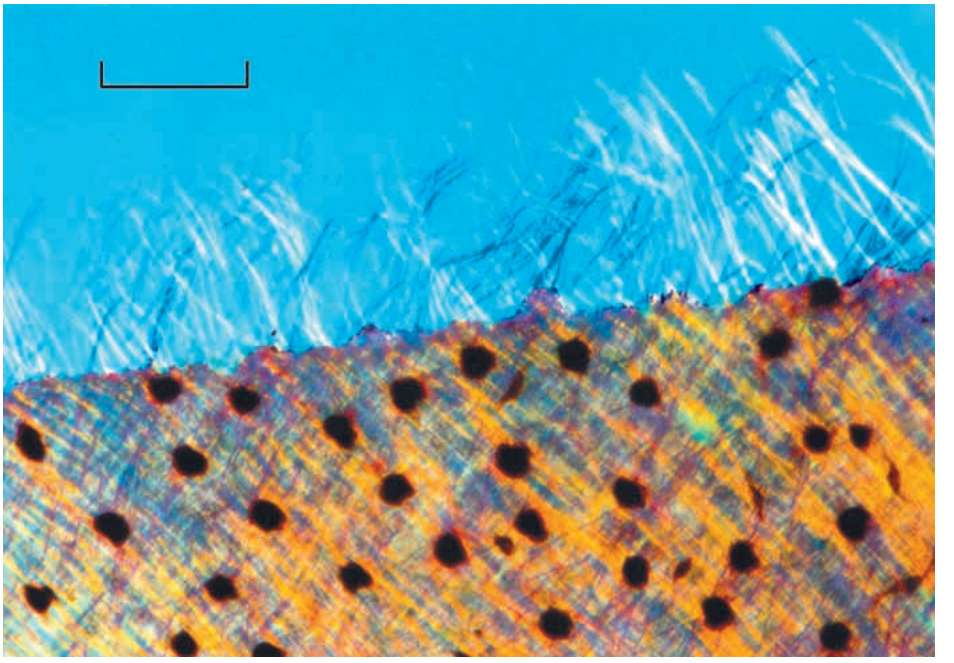

Fig. 4. Longitudinal sample of a split, whole tadpole tail fin viewed under birefringence microscopy and stained with Picrosirius Red. The longitudinal axis of the tail runs parallel to the exposed cut edge of the fin. The fin displays orthogonal layers of collagen fibres running at approximately ±45° to the longitudinal axis of the tail. Fibres can be seen projecting from the cut edge of the sample. The dark spots on the fin are pigment patches. Scale bar, 0.1 mm.

nevertheless had shortcomings. The fins still occasionally tore at the grips, and the samples also gradually elongated during loading and thus flexed (or sagged) when returned to zero extension. Both of these problems have previously been identified in tests of eel skin (Hebrank, 1980; Hebrank and Hebrank, 1986). Our samples failed in flexure during cyclic loading for preconditioning and testing. Indeed, several of the fin strips tore before all of the planned mechanical tests could be completed; hence, we report results for N=6 rather than N=10 for two of the tests. Although mounting and testing of vertically oriented fin strips was attempted, the tissue samples were too small to be held in the grips and still leave enough sample for testing.

In the present experiments, the maximum load that the tail fin could sustain in tension could not be established with any precision because of gripping problems, and the loads likely to be experienced by the fin in nature were unknown. Hebrank and Hebrank (1986) were similarly unable to assess the breaking strength of fish skin. We pragmatically chose a maximum load of 3 g for mechanical testing simply because the fins would not tolerate loads above 5 g. We noted that fin strips preserved in formalin were much stronger as a result of

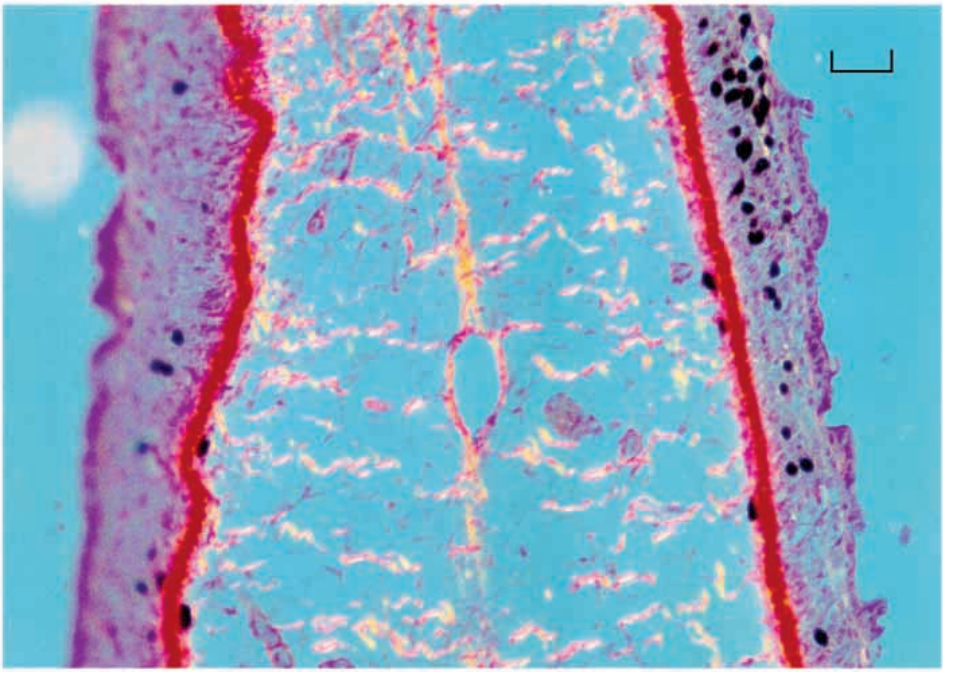

Fig. 5. Cross section of a formalin-fixed, paraffin-embedded tadpole tail fin, dorsal side up. The sample has been stained with Picrosirius Red to enhance birefringence. A thin sheath of highly birefringent collagen fibres lies under the epidermis and encloses a central region containing a gel-like material with loose connective tissue reinforcement. Scale bar, 0.1 mm.

collagen cross-linking and were able to tolerate loads of approximately 10 g.

Performing mechanical testing at such low loads also presented a problem because the equipment used was at its lower capability limits. At such low loads, the load data were visibly quantized by the A/D card. There was also noise associated with the load data, as seen in the stress–strain curves (Fig. 1).

The concave upward shape of the stress–strain curves found for tadpole tail fins is typical of other connective tissues. However, the fin demonstrates marked viscoelasticity as shown by the large hysteresis loss (Fig. 1; Table 1). The stress–strain response defines the relationship between load and extension in a material, normalized to eliminate the effects of specimen geometry. The area under a stress–strain curve is thus a measure of the work (strain energy) per volume required to extend a sample. In an elastic material, the mechanical energy required to deform the sample is stored as mechanical potential energy and is recovered as the sample returns to its initial dimensions. If the material is viscoelastic, some of the mechanical energy is lost as heat instead of being stored as potential energy and completely released (Denny, 1989). The per cent hysteresis calculated in the present study, for instance, represents the ratio of energy lost as heat to the total work done to extend the sample. This loss was a surprising 70 % in the fin, a value comparable with that presented by Hebrank (1980) for longitudinally tested eel skin. This contrasts markedly with the 15 % hysteresis loss found, for example, in bovine pericardium (Lee *et al.* 1994) tested using the same equipment and at the same frequency as in the present study. The stress–strain response therefore suggests that the tail fin is an extremely viscoelastic material.

Small-deformation forced vibration experiments were also performed to determine the fin's mechanical properties under small-amplitude excursions. In these experiments, the magnitude of the complex dynamic modulus $|E^*|$ represents the overall stiffness of the material in vibration. Correspondingly, (i) the storage modulus, E_S, is the elastic component of the dynamic modulus and (ii) the loss modulus, E_L, is the viscous component. In the present study, the mean dynamic modulus at 3 Hz was 293±42 kPa. Since the mean stress around which the tissue was vibrated sinusoidally during forced vibration was 6.95±0.38 kPa, the tangential modulus was also calculated from the large-deformation stress–strain curves at 7 kPa (85.1±6.5 kPa). Comparison of these moduli demonstrates that the fin is more than three times stiffer in small deformations. Because these tests were performed at a frequency that mimics the natural tail beat frequency of the tadpole (Hoff, 1987; Oxner *et al.* 1992), these results suggest that the fin may retain greater stiffness provided that the deformation is small. It is probably this property of the fin that contributes most to its ability to remain erect during active swimming despite the lack of any solid skeletal elements. The lower tangential modulus under large deformations may be due to greater shear thinning of the gel-like matrix within the fin during large fibre rotation towards the direction of stress (Lee *et al.* 1994).

The phase angle in forced vibration, ϕ, is indicative of the degree of viscoelasticity of the material since $\tan\phi$ is the ratio of the loss modulus to the storage modulus. A phase angle of 0 ° would be obtained with an ideal elastic material, whereas an angle of 90 ° represents the behaviour of a viscous Newtonian fluid. The mean phase angle of tail fins tested under forced vibration was 17.6±1.0 °, a value that indicates greater viscous behaviour than typically found in other connective tissues. For comparison, the human aorta has a mechanical function that depends on elastic storage of pulse pressure and is therefore considered to be a physiologically elastic material. It displays an approximate phase angle of 6.7 ° (Imura *et al.* 1990). Bovine pericardium similarly displays quite elastic behaviour with phase angles between 3 and 10 ° (Lee *et al.* 1994). We know of no other forced vibration data on fish or amphibian skin.

The viscoelasticity of the tadpole tail fin under large and small deformations was further demonstrated by stress relaxation. Stress relaxation refers to the decline in tensile stress that occurs over time when a material is held at a fixed length. After only 100 s of relaxation, 85 % of the initial stress in the fin had been lost through viscous processes. In contrast, bovine pericardium lost only 35 % of its initial stress over 100 s (Lee *et al.* 1994).

Some of the mechanical parameters for tadpole tail fin assessed herein can be compared with those for the only other anuran skin examined to date under uniaxial tension: namely that from adult *Xenopus laevis* (Greven *et al.* 1995). Adult *X. laevis* skin is much stiffer, with modulus values ranging from 10.4–12 MPa in females to 33.5–38.4 MPa in males. These values are fully two orders of magnitude greater than those obtained for the tadpole fin, reflecting the substantial collagen reinforcement of the adult tissue. In addition, the adult skin was highly extensible (63–102 % strain at failure *versus* approximately 10 % in the tail fin) and displayed considerable tensile strength (11–16 MPa) compared with the fragile tail fin tissue. The adult skin must be viscoelastic to some extent; however, Greven *et al.* (1995) neither assessed this behaviour nor commented on its influence in their experiments, perhaps because their tests were conducted in open air.

The exceptionally viscoelastic and fissile tail fin of tadpoles may have implications for the survival of these animals in nature. Tadpole tail tips and fins are often damaged by predators (Caldwell, 1982, 1994; Feder, 1983; Morin, 1985; Smith and Van Buskirk, 1995). The high incidence of tadpoles found in natural ponds alive, but with damaged fins (see above references; R. Wassersug, personal observation), suggests that tadpoles often escape total consumption even after being physically grasped by predators. Some laboratory studies suggest that tadpoles can sustain more than 25 % tail loss without a significant reduction in their ability to escape further predator attacks (Wilbur and Semlitsch, 1990; Figiel and Semlitsch, 1991), although a 75 % tail loss is clearly crippling to *Hyla chrysoscelis* tadpoles in staged encounters with *Tramea lacerata* naiads (Semlitsch, 1990). The precise amount of tail tip or fin that a tadpole can safely sacrifice to a predator

is likely to vary depending on the taxa and sizes of both predator and prey (see Travis *et al.* 1985).

A large variety of aquatic arthropods, including dragonfly naiads, water bugs, diving beetles, aquatic spiders and crayfish all prey on tadpoles (e.g. Caldwell *et al.* 1980; Gascon, 1992; Hews, 1988; Heyer *et al.* 1975; Lawler, 1989; Skelly, 1997; Werner, 1991, 1994). Unlike larger vertebrate predators, such as fish and turtles, which may chase tadpoles (e.g. Feder, 1983), invertebrate predators are largely 'sit-and-wait' predators. These animals lunge at their prey, stimulated mechanically and/or visually by movement (e.g. see Pritchard, 1965, on odonate predation). If one of these predators misses a tadpole's head-body, it is likely to hit the tip or edge of the tail. The viscoelastic flow characteristics of the tail fin may mean that the tadpole can pull its head-body away from the attacker, even while the fin remains within the clutches of the predator. The fin first stretches, flows and then either slips out or fails. The latter outcome leaves the tadpole with a lacerated fin (as witnessed by Morin, 1985; Caldwell, 1994), but otherwise intact. The highly viscoelastic nature of the tadpole tail fin may itself be an inevitable consequence of its fissile structure. A low volume fraction of collagen fibre support (see Fig. 5) will inevitably lead to dominance of the properties of the viscous gel/sol matrix: relaxation and flow. A more purely viscous or purely elastic fin might similarly allow the tadpole to pull away from the clasp of a predator, but would not necessarily be able to stay erect during active swimming.

When attacked by a large vertebrate predator, such as a turtle, that simultaneously grasps and dissects its prey with jaws, there may be little advantage to tadpoles in having viscoelastic tail fins. However, these same easily flowing fins may hinder certain invertebrate predators that must first grasp then subdue their prey before they initiate ingestion. The ability of the tadpole tail fin to stretch or flow will serve the tadpole most effectively when handling times for the predators are relatively long. Indeed, Kruse (1983) reported handling times of the order of seconds to minutes for predaceous diving beetles in staged encounters with tadpoles.

These observations alter our view of the tadpole tail fin as a strictly locomotor appendage. In addition to any role that the fin plays in locomotion, we suggest that it also acts as an expendable 'protective wrapping' around the important core muscle of the tail. The fin could keep the jaws and claws of potential predators from grasping the tadpole's muscle. By sacrificing its integrity to a predator and allowing the tadpole to escape, the tail fin may be analogous to the autotomized tail of many salamanders and lizards. A similar analogy can be made to the mere mouthful of feathers that a fox gets as a consolation prize for an unsuccessful foray into the chicken coop. In these situations, ostensibly locomotor structures, such as fins and feathers, may be sacrificed to save prey from otherwise lethal attacks.

The above speculation regarding the functional implications of the viscoelastic and fissile tadpole tail fin has implications for recently reported predator-induced polyphenism in tail shape for hylid tadpoles. In the presence of predaceous dragonfly larvae, tadpoles of several species develop a taller tail fin (Smith and Van Buskirk, 1995; McCollum and Van Buskirk, 1996, 1997; Bailey, 1997; McCollum and Leimberger, 1997) which, in certain circumstances, may improve their ability to flee from predators. Whereas the tail fin may help tadpoles to outswim their predators, our results suggest that this morphology may also help the same tadpoles to survive when fleeing fails and predators take hold of their tails.

We thank S. Waldman for assisting in the use of the analytical and computer hardware, and R. Khanna for developing the rubber-lined grips used to hold the tissue samples. N. Major helped with animal care and in the production of the final manuscript. In addition, J. Blair, M. Fejtek and J. Long read the manuscript in draft form and provided critical comment. We thank them all, as well as the Natural Science and Engineering Research Council of Canada, for their support of this research.

References

BAILEY, C. L. (1997). Performance of predator-induced morphologies in larval and recent metamorphs if the Pacific treefrog. *Am. Zool.* **37**, 200A.

BERNINGHAUSEN, F. (1997). *Welche Kaulquappe ist das? Der wasserfeste Amphibienführer*. Hannover: Naturschutzbund Deutschland (NABU).

CALDWELL, J. P. (1982). Disruptive selection: a tail color polymorphism in *Acris* tadpoles in response to differential predation. *Can. J. Zool.* **60**, 2818–2827.

CALDWELL, J. P. (1994). Natural history and survival of eggs and early larval stages of *Agalychnis calcarifer* (Anura: Hylidae). *Herpet. nat. Hist.* **2**, 57–66.

CALDWELL, J. P., THORP, J. H. AND JERVEY, T. O. (1980). Predator–prey relationships among larval dragonflies, salamanders and frogs. *Oecologia* **46**, 285–289.

CANADIAN COUNCIL ON ANIMAL CARE (1984). Amphibians. In *Guide to the Care and Use of Experimental Animals*, vol. 2, pp. 11–64. Ottawa.

DENNY, M. W. (1989). Invertebrate mucous secretions: functional alternatives to vertebrate paradigms. *Symp. Soc. exp. Biol.* **43**, 337–366.

FEDER, M. E. (1983). The relation of air breathing and locomotion to predation on tadpoles, *Rana berlandieri*, by turtles. *Physiol. Zool.* **56**, 522–531.

FIGIEL, C. R. AND SEMLITSCH, R. D. (1991). Effects of nonlethal injury and habitat complexity on predation in tadpole populations. *Can J. Zool.* **69**, 830–834.

FROLICH, L. M. AND SCHMID, T. M. (1991). Collagen type conservation during metamorphic repatterning of the dermal fibers in salamanders. *J. Morph.* **208**, 99–107.

GASCON, C. (1992). Aquatic predators and tadpole prey in Central Amazonia: field data and experimental manipulations. *Ecology* **73**, 971–980.

GOSNER, K. L. (1960). A simplified table for staging anuran embryos and larvae with notes on identification. *Herpetol.* **16**, 183–190.

GREVEN, H., ZANGER, K. AND SCHWINGER, G. (1995). Mechanical

properties of the skin of *Xenopus laevis* (Anura, Amphibia). *J. Morph.* **224**, 15–22.

HEBRANK, M. R. (1980). Mechanical properties and locomotion function of eel skin. *Biol. Bull. mar. Biol. Lab., Woods Hole* **158**, 58–68.

HEBRANK, M. R. AND HEBRANK, J. H. (1986). The mechanics of fish skin: lack of an 'external tendon' role in two teleosts. *Biol. Bull. mar. Biol. Lab., Woods Hole* **171**, 236–247.

HEWS, D. K. (1988). Alarm response in larval western toads, *Bufo boreas*: release of larval chemicals by a natural predator and its effect on predator capture efficiency. *Anim. Behav.* **36**, 125–133.

HEYER, W. R., MCDIARMID, R. W. AND WEIGMANN, D. L. (1975). Tadpoles, predation and pond habitats in the tropics. *Biotropica* **7**, 100–111.

HOFF, K. (1987). Morphological determinants of fast-start performance in anuran tadpoles. Thesis, Dalhousie University.

IMURA, T., YAMAMOTO, K., SATOH, T., KANAMORI, K., MIKAMI, T. AND YASUDA, H. (1990). *In vivo* viscoelastic behaviour in the human aorta. *Circulation Res.* **66**, 1413–1419.

KIER, W. M. (1992). Hydrostatic skeletons and muscular hydrostats. In *Biomechanics – Structures and Systems* (ed. A. A. Biewener), pp. 205–231. New York: Oxford University Press.

KRUSE, K. C. (1983). Optimal foraging by predaceous diving beetle larvae on toad tadpoles. *Oecologia* **58**, 383–388.

LAWLER, S. P. (1989). Behavioral responses to predators and predation risk in four species of larval anurans. *Anim. Behav.* **38**, 1039–1047.

LEE, J. M., HABERER, S. A., PEREIRA, C. A., NAIMARK, W. A., COURTMAN, D. W. AND WILSON, C. J. (1994). High strain rate testing and structural analysis of pericardial bioprosthetic materials. In *Biomaterials' Mechanical Properties* (ed. H. E. Kambic and A. T. Yokobori Jr), pp. 19–42. Philadelphia: ASTM.

LEE, J. M. AND LANGDON, S. (1996). Thickness measurement of soft tissue biomaterials: A comparison of five methods. *J. Biomech.* **29**, 829–832.

LIU, H., WASSERSUG, R. J. AND KAWACHI, K. (1997). The three dimensional hydrodynamics of tadpole locomotion. *J. exp. Biol.* **200**, 2807–2819.

MCCOLLUM, S. A. AND LEIMBERGER, J. D. (1997). Predator-induced morphological changes in an amphibian: predation by dragonflies affects tadpole shape and color. *Oecologia* **109**, 615–621.

MCCOLLUM, S. A. AND VAN BUSKIRK, J. (1996). Costs and benefits of a predator-induced polyphenism in the gray treefrog *Hyla chrysoscelis*. *Evolution* **50**, 583–593.

MCCOLLUM, S. A. AND VAN BUSKIRK, J. (1997). Individual behavioral and morphological traits as predictors of induced resistance to predators. *Am. Zool.* **37**, 93A.

MORIN, P. J. (1985). Predation intensity, prey survival and injury frequency in an amphibian predator–prey interaction. *Copeia* **1985**, 638–644.

OVERTON, J. (1976). Scanning microscopy of collagen in the basement lamella of normal and regenerating frog tadpoles. *J. Morph.* **150**, 805–824.

OXNER, W. M., QUINN, J. AND DEMONT, M. E. (1992). A mathematical model of body kinematics in swimming tadpoles. *Can. J. Zool.* **71**, 407–413.

PRITCHARD, G. (1965). Prey capture by dragonfly larvae (Odonata; Anisoptera). *Can. J. Zool.* **43**, 271–289.

ROSIN, R. (1946). Über Bau und Wachstum der Grenzlamelle der Epidermis bei Amphibien – Larven; Analyse eïner orthogonalen Fibrillärstruktur. *Rev. suisse Zool.* **53**, 133–201.

SEMLITSCH, R. D. (1990). Effects of body size, sibship and tail injury on the susceptibility of tadpoles to dragonfly predation. *Can. J. Zool.* **68**, 1027–1030.

SKELLY, D. K. (1997). Tadpole communities: pond permanence and predation are powerful forces shaping the structure of tadpole communities. *Am. Sci.* **85**, 36–45.

SMITH, D. C. AND VAN BUSKIRK, J. (1995). Phenotypic design, plasticity and ecological performance in two tadpole species. *Am. Nat.* **145**, 211–233.

TRAVIS, J., KEEN, W. H. AND JUILIANNA, J. (1985). The role of relative body size in a predator–prey relationship between dragonfly naiads and larval anurans. *Oikos* **45**, 59–65.

TURNER, S. (1983). *Mechanical Testing of Plastics*, pp. 12–40. Harlow, UK: G. Godwin.

VESELY, I. AND BOUGHNER, D. R. (1985). A multipurpose tissue bending machine. *J. Biomech.* **18**, 511–513.

WAINWRIGHT, S. A., BIGGS, W. D., CURREY, J. D. AND GOSLINE, J. M. (1976). *Mechanical Designs in Organisms*. London: Edward Arnold.

WASSERSUG, R. J. (1989). Locomotion in amphibian larvae (or 'Why aren't tadpoles built like fish?'). *Am. Zool.* **29**, 65–84.

WASSERSUG, R. J. AND HOFF, K. (1985). The kinematics of swimming in anuran larvae. *J. exp. Biol.* **119**, 1–30.

WERNER, E. E. (1991). Nonlethal effects of a predator on competitive interactions between two anuran larvae. *Ecology* **72**, 1709–1720.

WERNER, E. E. (1994). Ontogenetic scaling of competitive relations: size-dependent effects and responses in two anuran larvae. *Ecology* **75**, 197–213.

WILBUR, H. M. AND SEMLITSCH, R. D. (1990). Ecological consequences of tail injury in *Rana* tadpoles. *Copeia* **1990**, 18–24.

YOSHIZATO, K. (1986). How do tadpoles lose their tails during metamorphosis? *Zool. Sci.* **3**, 219–226.